A Comparative Study of Metrology Techniques for Porous Organic Thin Films

by

Yee Lam

S.B. Materials Science and Engineering, 2001
Massachusetts Institute of Technology

Submitted to the Department of Materials Science and Engineering
in Partial Fulfillment of the Requirements for the Degree of
Master of Science in Materials Science and Engineering

at the

Massachusetts Institute of Technology

June 2002

Signature of Author:_____
Department of Materials Science and Engineering
May 10, 2002

Certified by:_____
Eugene A. Fitzgerald
Professor Materials Science and Engineering
Thesis Supervisor

Accepted by:_____
Harry L. Tuller
Professor Materials Science and Engineering
Chairman, Committee for Graduate Students

A Comparative Study of Metrology Techniques for Porous Organic Thin Films

by

Yee Lam

Submitted to the Department of Materials Science and Engineering
on May 10, 2002 in Partial Fulfillment of the
Requirements for the Degree of Master of Science in
Materials Science and Engineering

ABSTRACT

With the development of porous materials for use as dielectrics in microelectronics processing, appropriate metrology tools are needed to monitor and characterize the pore size, distribution, and percent porosity in these films in an industrial setting. Techniques used to characterize and monitor porosity in thin films are oftentimes destructive, such as Transmission Electron Microscopy and Scanning Electron Microscopy; indirect, such as optical ellipsometry and X-Ray Reflectivity; or pose problems for industrial use, involving radioactivity such as Positronium Annihilation Lifetime Spectroscopy and Small Angle Neutron Scattering. Atomic Force Microscopy is limited to surface analysis, and pores may be intersecting the surface at a variety of chords, not necessarily the diameter. Each of these techniques also has unique advantages, and a combination of these techniques can compensate for limitations such as inability to detect closed pores or constraints on pore size range of measurement. The following study is a round robin evaluation of these techniques using Developmental (Version 7) Porous SiLK™ from DOW Chemical (Midland, MI) manipulated to create pores of varying sizes. Optical tools and a possible inline X-Ray Reflectivity tool were found to be optimal for implementing porosity characterization in industry, since both techniques are commercially available, have proven high throughput, and can be clearly correlated to pore size and porosity in organic thin films.

Thesis Supervisor: Eugene A. Fitzgerald
Title: Professor of Materials Science and Engineering

Acknowledgements

This study was the collaborative effort of people at Advanced Micro Devices (Sunnyvale, CA), The DOW Chemical Company (Midland, MI), The University of Michigan (Ann Arbor, MI), and The Massachusetts Institute of Technology (Cambridge, MA).

From AMD, many thanks to Suzette Pangrle for her mentorship and technical guidance, making this project both educational and enjoyable, and Nick Tripsas for his support and industrial know-how, making this project possible. Thanks to Alex Nickel and Hieu Pham for the many discussion sessions and struggles with tools, and to Stephen Robie for his technical advice. Thanks also to Jonnie Barragan and Jerry Romero for their technical assistance. From the DOW Chemical Company much gratitude to Carol Mohler and Don Frye for their input and assistance. From the University of Michigan, many thanks to David Gidley, Jianing Sun, Yifan Hu, and the rest of the Positron group for their time, effort, and expert guidance. From the Massachusetts Institute of Technology, thanks so much to Eugene Fitzgerald for his optimism and guidance.

Lastly but not leastly I must thank my father, Tung-Shing Lam, mother, Lai-Wan Yuen, and brothers Yik and Yeung Lam for all the countless things they have done to make this possible. And to Rob Pinder, Caroline Rhim, and Siu Ho, thanks for the encouragement, endless support, and sense of humor through it all.

Thank you.

Table of Contents

List of Figures

Page number

List of Tables

Page number

1. Introduction

Developments in lithography have advanced the microelectronics industry past its current feature size limitations. New challenges, however, must now be met by the materials which will be used to create these features. Cross talk between metal lines and the interconnect Resistance-Capacitance (RC) time delay (τ) are becoming the major limitations to increasing device speed. For the past decade, the industry has focused efforts on decreasing the resistance by utilizing copper technology. Success in copper integration has allowed new efforts to decrease the capacitance by investigating new low dielectric constant materials to facilitate the improvements in design.

One key material in this framework is the inter-layer dielectric (ILD), which is largely responsible for the capacitance in the RC delay. Current technologies rely on a silicon dioxide (SiO_2) layer, with a dielectric constant (κ) of approximately 4.0 to act as the dielectric. Within the last five years, lower κ materials have been developed to reduce the charge buildup with κ values at or below 3.0. These new materials are mostly silica based with organic dopants, or in the case of DOW Chemical's SiLK™, completely organic. These materials, however, are not as well matched as SiO_2 to the silicon substrate, and consequently suffer thermal, mechanical, and uniformity properties inferior to SiO_2.

Building on technology from these low κ materials, lower κ values have been achieved by inducing nanoscale porosity into these films, resulting in dielectric constants at or below 2.0. Porosity will not only lower the κ value, however, but will also cause further changes in mechanical and thermal properties. Porosity can also introduce problems during processing, as interconnected voids can increase diffusion in etch and plasma processes, and surface pores can lead to discontinuities in the barrier layer. For these reasons, porosity must be closely monitored in these thin films. Metrology must be modified or created to analyze the unique structures of these films, since existing tools have not been used to analyze nanoporous thin films. Current techniques used to characterize and monitor porosity are oftentimes destructive, indirect, or not practical for industry. Also many techniques are only able to detect interconnected pores. In order to explore metrology for the next generation ILD, the following study will use developmental version 7 porous SiLK™ from DOW Chemical to evaluate the techniques

available and suggest a viable combination for implementing porosity characterization in industry.

2. Background

2.1 Inter Layer Dielectric

Dielectric materials in the semiconductor industry are used to insulate metal lines or devices, reducing cross talk between them, and decreasing leakage current. Figure 2.1 shows an image of the interlayer dielectric (SiLK™ from DOW Chemical) in a copper dual damascene integration scheme. [IMEC, Hitachi].

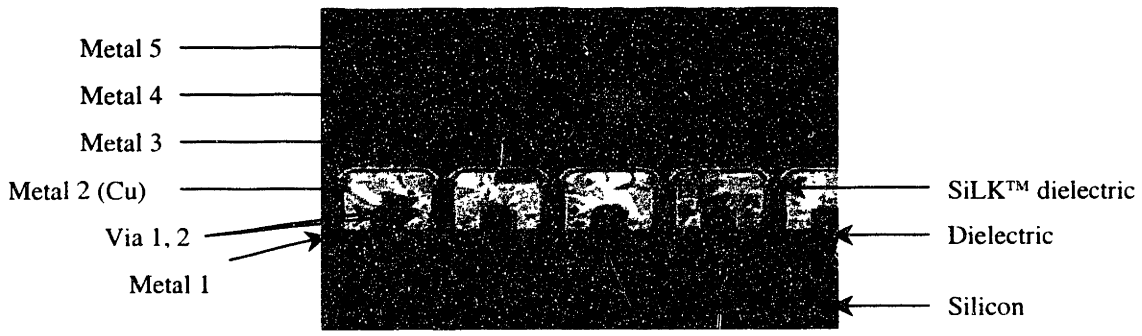

Figure 2.1 Cross-sectioned scanning electron micrograph of SiLK™ dielectric in copper dual damascene integration scheme. (Courtesy of IMEC, Hitachi)

Since early silicon device and circuit development, silicon dioxide (SiO_2), a native oxide, has been the standard dielectric. Advances in lithography, etch specificity, and other aspects of semiconductor processing have spurred the development of new materials. These materials must provide adequate insulation while decreasing the dielectric constant to reduce capacitance time delay, which is the minimum time necessary to charge and or discharge a metal interconnect, as well as cross talk between the interconnects. Interconnect line resistance capacitance time delay can be related to the dielectric constant by the following equation:

$$\tau_{RC} = 2\rho\kappa\varepsilon_0 (4L^2/P^2 + L^2/T^2)$$

where ρ is the resistivity of the material, κ the dielectric constant, ε_0 the permittivity of free space, L the interconnect line width, P the metal pitch, and T the metal thickness.

Due to this proportional relationship, a decrease in κ will result in a decrease in the RC delay. [Lee, Ho], thus allowing faster circuit operation.

According to the International Technology Roadmap for Semiconductors, the interlayer dielectric will need to have an effective dielectric constant of 2.6 within the next 2 years, and 2.1 within the next 10 years. [ITRS, 2001] The effective dielectric constant is a measurement of the integrated film stack including the low κ material, capping layer, and diffusion barrier, etc. This effective value yields more realistic data for an integrated device than does data for the material alone. These materials are mostly silicon based with organic dopants or purely organic, and porosity has been induced to further reduce the κ value. Considerations in determining the optimal material do not only depend on the κ value, but also on the change in mechanical strength, which greatly affect chemical mechanical polishing in later steps, thermal conductivity, and electrical properties such as leakage current. Methods to lower κ value are outlined below in figure 2.2 [Toma]

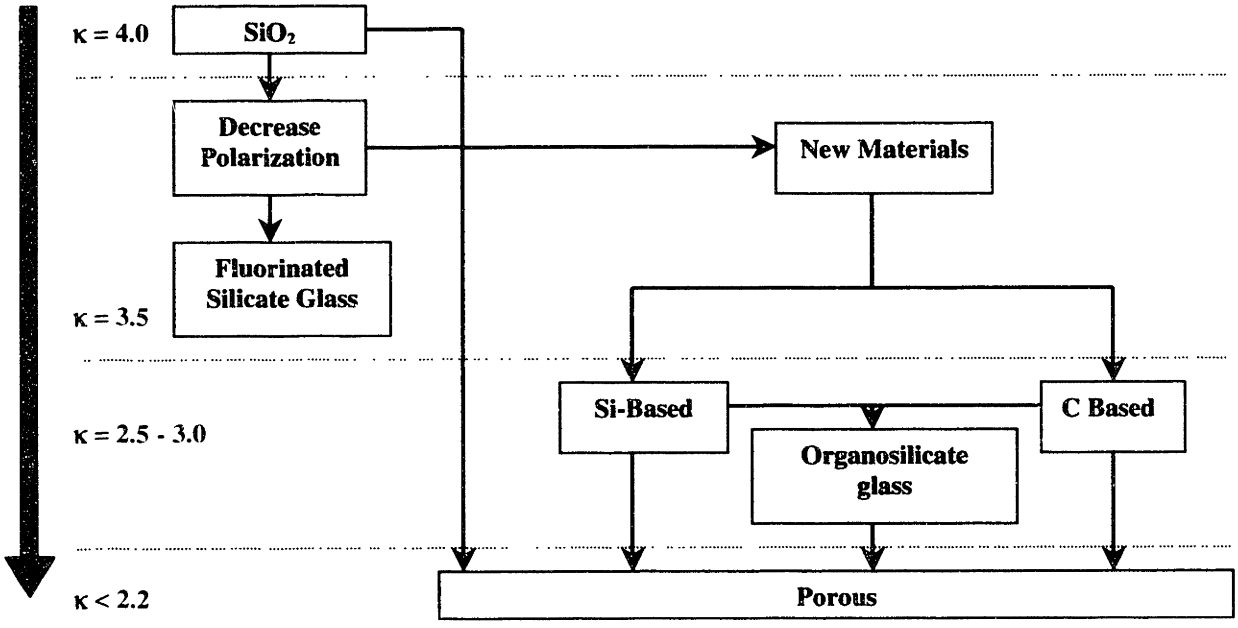

Figure 2.2 Methods of lowering κ value, incorporating new materials deposited through spin on and chemical vapor deposition methods. [Toma]

2.2 SiLK™

Several porous low κ materials have been under development to meet the quickly changing needs of the semiconductor industry. DOW Chemical's SiLK™ is a completely organic compound, which is processed in three steps. The first step is a spin coat which drives off the low temperature solvent, then a low temperature bake drives off the higher temperature solvent, and the final step is a high temperature cure where the polymer matrix is cross linked as shown in Figure 2.3. The polymer is then stable in air and can continue into the patterning process.

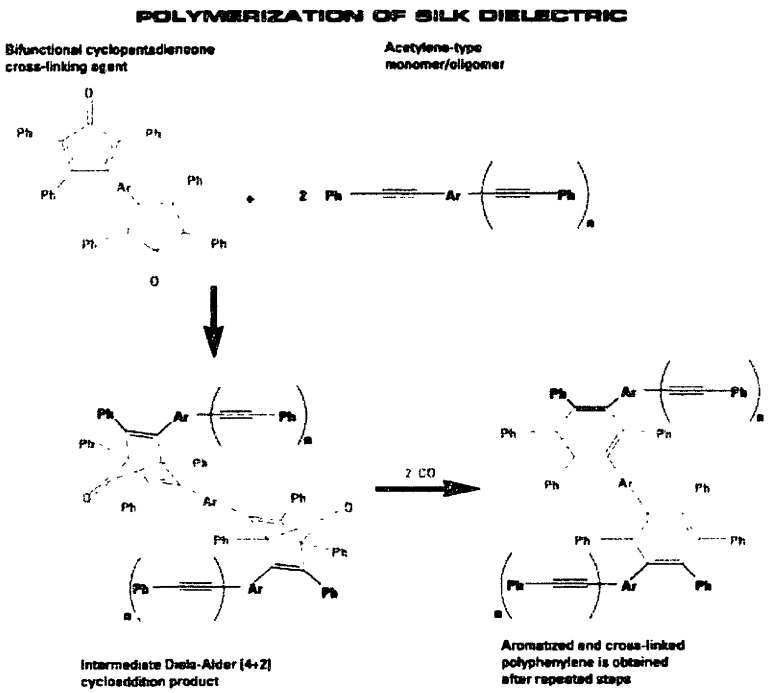

Figure 2.3 Polymerization of dense SiLK ultra low κ dielectric. (κ ~ 2.65) [Golden]

DOW has been working to advance this technology, further decreasing the dielectric constant by incorporating mesopores (pore diameter between 20Å and 500Å) into the organic matrix. Another organic molecule is bound to a percentage of the SiLK monomers. During the cure step, this molecule will decompose and diffuse through the matrix, acting as a sacrificial porogen. Each porogen molecule, or aggregation of porogen molecules leaves a roughly spherical void, which translates into a closed pore system with a distribution of pore sizes. The material has shown thermal properties similar to those of dense SiLK, but mechanical properties vary with porosity.

2.3 Porosity Effects

Porosity has long been a concern in the field of thin films, particularly in the microelectronics industry. Previously pores were often seen as defects, and defect analysis was effective in monitoring pore size. As devices scale to 100nm, however,

porosity is purposely introduced into the dielectric layer. Therefore the pore diameter must be carefully monitored to ensure final film properties will meet needed specifications. κ values below 2.5 are difficult to achieve with dense inorganic or organic materials, but introducing pores into these films may lower the κ to as low as 1.1 as κ scales directly with density. [Jain] Greater porosity will decrease the κ value according to the Bruggeman Equation below:

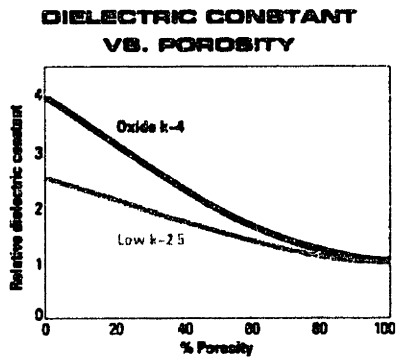

Figure 2.4 Dielectric constant versus porosity, showing an approximately linear relationship between the two variables. Materials with larger dielectric constants (i.e. SiO_2 κ~4.0) will require more porosity to achieve the same κ values as materials with lower starting κ values (i.e. SiLK k~2.65). [Golden]

$$f_1 \frac{(\kappa_1 + \kappa_e)}{(\kappa_1 + 2\kappa_e)} + f_2 \frac{(\kappa_2 - \kappa_e)}{(\kappa_2 + 2\kappa_e)} = 0$$

where $f_{1,2}$ represent the fraction of the components (matrix and pores (air) respectively), $\kappa_{1,2}$ the dielectric constant of the components, and κ_e the effective dielectric constant of the porous material. [Morgan] Figure 2.4 shows that materials with larger dielectric constants (i.e. SiO_2 κ~4.0) will require more porosity to achieve the same low κ values as other materials with lower starting k values (SiLK κ~2.65).

While decreasing the dielectric constant in these thin films, the mechanical and thermal properties are also affected by the increasing porosity. Porous SiLK is a closed pore structure with generally spherical voids. As the porosity is increased, however, the number of pores can reach the percolation limit, where the volume of the second component (air voids) becomes large enough to create small, interconnected areas. This process can cause the final film to begin showing characteristics of an interconnected pore network. This geometric aspect of the porosity also plays a part in final film properties. Interconnected pores facilitate any diffusion of etch or other processing chemicals into the film, while closed pores prevent these larger molecules from diffusing into the layer. Conversely, interconnected pores better facilitate the escape of any trapped species resulting from processing. Pore size also plays a large role in future integration, as large pores can cause discontinuities in thin barrier layers deposited on the surface as in figure 2.5. [Sun] For this reason, pore sizes should be on the order of one tenth the feature size, or about 10 nm, for the 100 nm technology node.

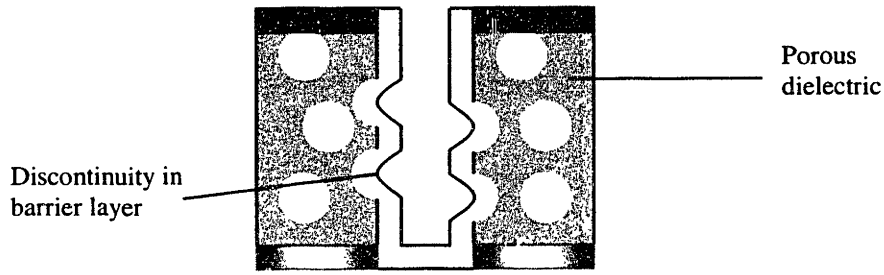

Figure 2.5 Barrier metal not continuous due to large (> 10 nm) pores on surface of etched feature.

2.4 Metrology Techniques

Metrology is an integral component in developing these low k films for large-scale integration, as monitoring must be done after the film deposition and curing steps to ensure a film which meets specifications for future properties. These metrology tools will eventually need to function in a fabrication facility line, meeting class one clean room (1 ppm) restrictions. A solution is to modify a tool already being used in-line, such as an optically based reflectometer or ellipsometer to determine the index of refraction and thickness of different films. The refractive index (n) of a porous material is the weighted average of the film matrix index (n>1) and air (n=1). The matrix will have a much higher index than the air-filled pores. Hence a porous version of the matrix will have a lower effective refractive index than the original dense matrix. In order to apply this in determining the porosity or pore size, however, these data must be correlated with another technique to calibrate the tool. Calibration techniques need not be in-line, and can therefore be modifications on existing laboratory equipment.

2.4.1 Porosity Determination

2.4.1.1 Optical Methods

Many tools in thin films analysis utilize spectroscopic ellipsometry to determine the optical properties and thickness. In this technique, a monochromatic beam of light is reflected from a material surface at a non-normal angle, and causes a polarization change which can be recorded and related to the index of refraction. [Collins] These measurements are very sensitive to the wavelength of the beam, however, and data is relative to this wavelength.

Studies performed with varying porous materials have determined a linear relationship between the refractive index and porosity. One such study using a nanoglass material (porous SiO_2) concluded film porosity by comparing the refractive indices of samples with varying porosity to the dense sample. The relationship between void fraction and refractive index was indeed linear. [Srivasta] Using porous SiLK, the experiment also showed a linear correlation.

2.4.1.2 Ellipsometric Porosimetry

Traditional methods involving gas adsorption and diffusion have long been used to measure porosity in thicker films, but have been unsuccessful with nanoporous thin films. These methods rely on diffusing nitrogen into a film and decreasing the temperature to approximately 77K to condense N_2 in the pores. The partial pressures of gas adsorbed in the pores are then used to calculate pore sizes and porosity. [Baklanov, 2001] This technique requires interconnected pores as well as greater pore volumes to allow the nitrogen to diffuse, limiting effective measurement of closed pore thin films.

An improvement on this technique to measure pores in thin films employs a solvent which diffuses through the interconnected pore network, and measurements of index of refraction are taken using optical methods. This data is then compared for samples with and without the injected solvent to determine the size and percentage of interconnected pores. This value is subtracted from the total porosity determined by comparing the refractive index of the dense to porous material, to determine the percentage of interconnected porosity. Pore sizes can only be determined for interconnected pores, using the Kelvin equation below:

$$1/r_1 + 1/r_2 = - RT/(\gamma V_L \cos\theta) \ln P/P_0$$

where r_1 and r_2 define pore sizes, R is the gas constant for the solvent, γ and V_L are the surface tension and molar volume of the adsorbate respectively, θ is the contact angle of the adsorbate, and P_0 is the partial pressure of the system vs. the P for the solvent.

Assuming $r_1 \sim r_2 \sim r$, this yields an equation for the pore radius:

$$r = (2\gamma V_L)/[RT \ln (P/P_0)]$$

In order to use the Kelvin equation, it must be assumed that the pore size is much smaller than the probe diameter, and that the chemical potential is lower in the pore, the decreased potential being directly proportionally to the mean curvature of the surface separating the condensed material from the vapor. [Brown] In measuring thin films, using large molecules such as toluene or hexane will limit the resolution of pore size measurement. [Baklanov, 2000] This method has been shown promise with many organic doped silica low κ materials, but a suitable solvent has not yet been found for a purely organic film, as organic solvents swell the cross-linked polymer, distorting the original pores. Research is ongoing to develop a suitable solvent for organic films.

2.4.1.3 X-Ray Reflectivity

X-Ray Reflectivity is another standard metrology tool that has also been modified to characterize porosity in thin films. Data can be converted to determine the density, thickness, and surface roughness of a thin film, as well as the interfacial roughness between the film and substrate or two films in a multi-layer stack. [Bontempi]. X-rays are directed to the surface of the film at a small incidence angle, and the resulting data is graphed as the percentage maximum intensity (reflectance) versus incident angle. The rates at which the intensity amplitude decreases, and the overall decrease are both a function of surface and interfacial roughness. Below the critical angle, x-rays reflect off the sample surface at approximately 100% efficiency. Above the critical angle, x-rays begin to penetrate into the film. The density of the film can be calculated using a software package based on the proportional relationship between the critical angle and the square root of the density. The calculated density can then be converted into a measurement of porosity based on a comparison of the porous and dense material using the following equation:

$$P = 1 - (\rho_{porous}/\rho_{dense})$$

where P is the porosity, and ρ the densities of the respective materials.

2.4.1.4 Small Angle Neutron and X-Ray Scattering

Small angle scattering encompasses techniques using neutrons, x-rays, and light, where radiation is elastically scattered by a sample. Raw data, in terms of reflected intensity and scattering angle, can yield information about the pore size and shape. Neutrons and x-rays are most useful in the porous thin film regime, as the resolution is between 0.1 and 1000 nm [King], and pore diameters range from 3-100 nm.

Neutrons and x-rays both scatter within the desired length scale, but they differ on an atomistic level in the mechanism by which they interact with the film surface. Neutrons are scattered by atomic nuclei, while x-rays are scattered by electrons surrounding the nuclei. Due to this phenomenon, small angle neutron scattering is much more sensitive to composition, able to detect differences in isotopes in the material, while x-rays can only differentiate between materials of different elements. [King] In monitoring organic porous films, this additional sensitivity may also be very useful since organics often have a relatively low electron density.

Analysis with small angle neutron scattering (SANS) requires a neutron source, either nuclear fission of uranium-235 or spallation techniques, where a high-energy proton beam can shatter the nucleus, releasing neutrons. [Baklanov, 2001] This technique generates a plot of scattered neutron intensity (I) versus the scattering vector (q), where $q = (4\pi/\lambda) \sin(\theta/2)$. θ is the scattering angle from the incident beam path, and λ is the neutron wavelength (6Å). This q value is also a function of the porosity and wall density, which can be correlated to pore size. Small angle x-ray scattering (SAXS) functions similarly, with different relationships between the intensity and sample porosity and pore size. [Baklanov, 2001] X-rays are much easier to generate, so this technique can be more easily integrated into a laboratory or fabrication facility.

SANS has been shown most successful in analyzing pores larger than 10 nm, but studies using both small angle neutron scattering (SANS) and small angle x-ray scattering (SAXS) have shown data comparable to that using other techniques discussed in this study. [Baklanov, 2001] Data was not collected on the porous SiLK samples in this study due to tool unavailability during the time of experiment. Future analysis using SANS and SAXS will be very useful in validating data from this study, as well as determining viable options for inline monitoring.

2.4.2 Pore Size Determination

2.4.2.1 Positronium Annihilation Lifetime Spectroscopy

Positronium Annihilation Lifetime Spectroscopy (PALS) also utilized an adsorbate in the pores, but unlike porosimetry, the adsorbate is not a gas or solvent, but a positron. This positively charged electron binds with free electrons in the polymer matrix to form a neutral positronium complex (Ps) as it diffuses through the dense matrix. The natural vacuum lifetime of a Ps complex is 142 ns, [Gidley] however it will annihilate to gamma radiation at a shorter time when in a confined, or closed, pore. This decreased lifetime varies with surface area, or size, of the pore, since it is due to collisions with the pore surface, more quickly breaking the complex into gamma radiation. [Goworek] In a closed pore system, this information will yield a pore size distribution. In an interconnected pore network, the sample can be coated with an alumina or silicon dioxide surface to prevent escape of the Ps, and the data will yield an average pore size. PALS has shown to be sensitive to pore size determination in a range between 0.3 nm and 30 nm. The larger limit to pore size determination is set by the vacuum lifetime, where pores larger than 30 nm are hard to distinguish from Ps escaping into vacuum. [Gidley]

This technique has shown success with at least partially interconnected porous siloxane spin on glass materials, such as nanoglass, XLK (DOW Corning, Midland MI), and IPS (Catalysts and Chemicals Industry Corporation, Ltd., Japan) [Baklanov, 2001], and shows promise for closed pores, as positrons and Ps can diffuse relatively easily through the dense matrix. SiLK, however, may pose challenges due to the low electron density in organic molecules. Low numbers of larger pores can also pose problems, as Ps will not be able to diffuse as easily through the matrix before annihilating in micropores.

Depth profiling can also be achieved using this technique by varying the positron beam energy according to the following equation:

$$D = 0.7\ (400\ \text{Å} / \rho)\ E^{1.6}$$

where D is the mean implantation depth (Å), ρ the film density (g/cm^3), and E the beam energy (keV). Higher beam energies implant more positrons into the substrate, while

lower beam energies are more likely to backscatter off the surface. This backscattering generates background noise for each measurement, and must be subtracted from the total intensity signal. [Gidley]

2.4.2.2 Atomic Force Microscopy

Atomic Force Microscopy (AFM) has long been used to create topographical images of film surfaces. A silicon or silicon nitride tip mounted on a cantilever is slowly dragged across the surface in one of three modes: tapping, contact, or non-contact. Due to the delicate nature of thin films, tapping mode is most commonly used, and the cantilever makes contact with the sample in a sinusoidal pattern, causing little damage to the surface.

Analysis of copper grains has shown good resolution at the 10-20nm length scale for surface features, which is approximately that of the desired pore sizes. Success has also been demonstrated with copper surfaces that power spectral density function can be performed on an AFM image to determine the grain sizes. [Lita] When used on the surface or cross section of a porous thin film, data from an AFM image yields pore size as well as pore size distribution in the film both radial and circumferential. These outputs suggest that this technique may be useful in determining surface pore diameters.

3. Methodology

In order to calibrate an optically based in-line tool to determine pore size and porosity, porous 3000 Å SiLK (pSiLK) experimental version 7 with the same percentage of porogen loading was spun onto a set of silicon wafers. Two wafers each were processed in five different conditions to manipulate the pore size and distribution in the film. As a control, two silicon wafers were coated with 950 nm SiO_2, 50 nm Si_3N_4, and approximately 3600 Å dense SiLK processed with standard the procedure from DOW Chemical. These fourteen samples were then measured using a Therma-Wave Opti-Probe 2600DUV tool with appropriate recipes to determine the refractive index and thickness of the films. Next they were imaged using scanning electron microscopy (SEM) and transmission electron microscopy (TEM). Pore sizes were manually measured from the

images and used as baselines for calibrating data from Positronium Annihilation Lifetime Spectroscopy (PALS), Atomic Force Microscopy (AFM), and X-Ray Reflectivity (XRR). A capacitance measurement was also taken on each sample to determine the κ value.

3.1 Scanning Electron Microscopy Procedure

The samples were first plated with platinum for 1 minute in the 20 to 30 mA range using a Denton Vacuum model DESK II plater. This plated layer acted as a conductive coating to the top the sample to avoid sample charging while viewing in the SEM. A 5x5 μm platinum square was then deposited onto the samples in the SEM using the e-beam in a dual beam Focused Ion Beam (FIB) (FEI Company, Model DualBeam 820) at 3kV. In addition to this layer, a second layer was deposited over the same area using the ion-beam platinum of the same tool at less than 70pA. The final thickness of these last two layers was approximately 4000Å to 5000Å. These platinum layers acted as a protective coating over the pSiLK. The samples were then cross-sectioned using a standard FIB cut (rough cut at approximately 300pA and finish cut at 150pA). The samples were then coated with gold or platinum viewed in a Philips XL50 SEM operating at less than 2kV.

3.2 Transmission Electron Microscopy Procedure

The samples were first coated with 1 nm of chromium using a high-resolution sputter coater, Denton HiRes 100. The chrome layer acted as a marker on the surface of the porous SiLK film during later TEM examination. The Cr coated pSiLK film was then scraped off the silicon wafer and sandwiched between two epoxy blocks to be placed in a microtome chuck. The sample chuck was then placed in an ultra microtome to produce 30 nm sections. After drying the samples were examined using a Philips CM12 TEM operating at 120 keV. The image was then acquired using a Gatan Multiscan (model 794) camera.

3.3 Positronium Annihilation Lifetime Spectroscopy Procedure

The samples were placed in a vacuum chamber pumped down to 10^{-7} torr. A radioactive ^{22}Na β^+ source generated positrons for an electrostatically focused beam set at 3.1 keV (~1700 Å into the surface). The beam was focused on the samples, which were left to run for 12 hours while the resulting gamma radiation was captured by a detector in increments of microseconds. In order to depth profile the film, this procedure was then repeated for each sample at 2.1 keV (~920 Å) and 4.1 keV (~2700 Å). This data was then converted to lifetimes by timing electronics. The lifetimes were fitted to pore sizes using POSFIT® software generating a best fit with 2 discrete lifetimes.

3.4 Atomic Force Microscopy Procedure

The samples were analyzed using a Digital Instrument Dimension 5000 Atomic Force Microscope. The silicon tip was attached to an aluminum-coated cantilever with a nominal diameter of approximately 50Å. The tool was operated in tapping mode at a tip resonating frequency of approximately 300 kHz at a scan rate of 0.7 – 1.0 Hz.

3.5 X-Ray Reflectivity Procedure

Porous SiLK Samples processed under each condition as well as the dense sample were analyzed using a Philips X'pert PRO MRD four axis diffractometer with an additional x-y-z sample stage. The triple axis high resolution optics were used to produce a single incident wavelength which minimize the intensity between adjacent fringes, producing the sharpest critical angle. The incident beam optics used were a 4-bounce Ge (220) Bartels Monochromator and a crossed slit collimator (2mm wide, 5 mm high). The diffracted beam optics used were a 3-bounce Ge (220) triple axis monochromator and sealed Xe/Methane proportional x-ray detector. After aligning the sample, it was scanned using a scan range of 0.001 to 1.999, a step size of 0.002, and a step time of 1 second. The X-ray power was set to 45kV and 40 mA. The raw data was then modeled using Rigaku® software.

3.6 Capacitance Measurement

The capacitance of each sample was measured using a Four dimensions, Inc. C-V Map. This tool uses a mercury probe technique to generate C-V and I-V characteristics of the sample. The capacitance was then converted into a dielectric constant using the following equations.

[1] $\varepsilon_{tot} = (C_{tot}) * (\text{Thk low } \kappa + \text{oxide}) / (\text{Hg dot size}) / 100000$ [e-12 F/m]

[2] ε_f (low κ) = (Thk low k) / [(Thk low κ + oxide) / (ε_{tot}) - (Thk oxide) / ε_t)] [e-12 F/m]

[3] $\kappa = \varepsilon_f / \varepsilon_0$

where ε_{tot} is the total permittivity of the film stack, Hg dot size = 0.01372 cm^2, ε_f is the permittivity of the low κ material, ε_t is the permittivity of SiO_2 = 33.823 e-12 F/m, ε_0 is the permittivity of free space = 8.854 e-12 F/m, C_{tot} is the total capacitance from the Hg Probe measurements [e-11 F], and Thk low κ is the thickness measurement from the optical tool [Å].

4. Results

4.1 Optical Data

Data from the Opti-Probe are shown below in Table 4.1. Fourteen samples processed at different conditions measured using the Opti-Probe 2600 DUV. Thickness (Å), thickness non-uniformity at 1 σ (%), refractive index (RI), and RI non-uniformity also at 1 σ (%) were recorded. Goodness of Fit (GOF) from an Opti-Probe measures the agreement between measured data and a mathematical model based on pre-assigned values for thickness and refractive index.

Table 4.1 Values from spectroscopic ellipsometry for thickness, refractive index (RI), and goodness of fit (GOF)

Sample	Thickness	Thk NonUnif	RI	RI NonUnif	GOF
	(nm)	1 σ (%)		1 σ (%)	
Dense SiLK J					
0	361.51	0.75	1.6411	0.47	0.9859

Table 4.1 continued Values from spectroscopic ellipsometry for thickness, refractive index (RI), and goodness of fit (GOF)

Sample	Thickness	Thk NonUnif	RI	RI NonUnif	GOF
	(nm)	1 σ (%)		1 σ (%)	
Trend Matrix (pSiLK v7)					
A	311.49	0.33	1.5468	0.19	0.9678
B	313.58	0.25	1.5470	0.23	0.9646
C	313.91	0.43	1.5534	0.27	0.9495
D	312.50	0.40	1.5704	0.26	0.9343
E	303.08	0.42	1.5683	0.24	0.9763

4.2 Scanning Electron Microscopy

SEM images are shown below for the six SiLK samples in figure 4.1 below.

Sample 0

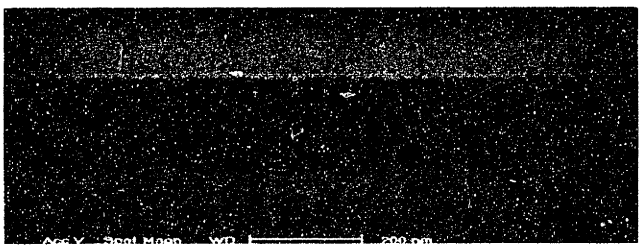

Sample A

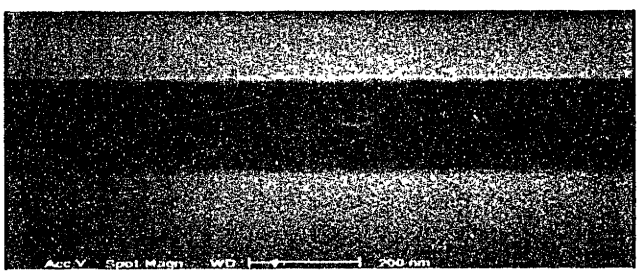

Sample B

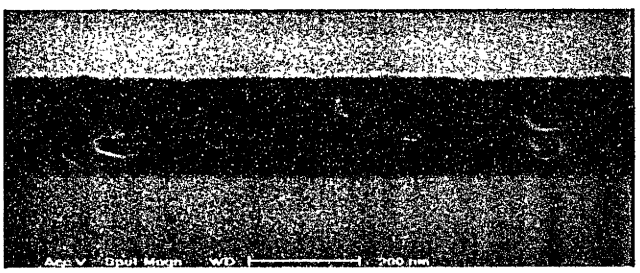

Sample C

Figure 4.1 SEM images of cross-sectioned samples for the dense SiLK sample (0) as well as the five porous samples (A-E).

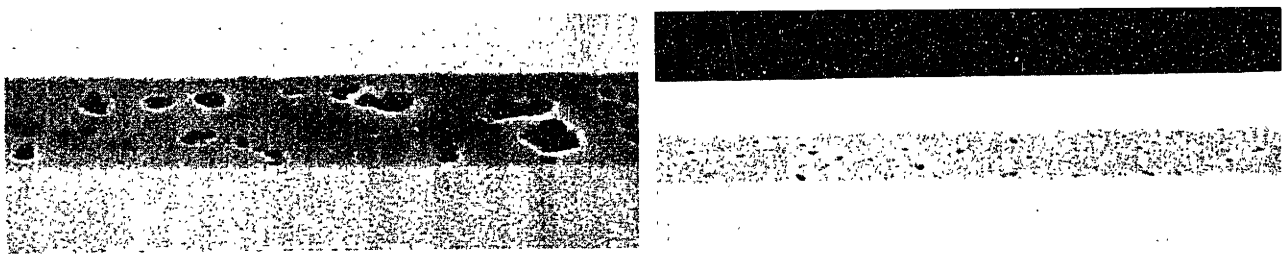

Sample D Sample E

Figure 4.1 continued. SEM images of cross-sectioned samples for the dense SiLK sample (0) as well as the five porous samples (A-E).

Manual pore size measurements to determine average pore size and pore size range in the image are shown in table 4.2.

Table 4.2 Manual pore size measurements for each sample from the previous SEM images.

Sample	Pore size range (nm)	Avg pore size (nm)	Sample	Pore size range (nm)	Avg pore size (nm)
Dense SiLK J			Trend Matrix (pSiLK v7)		
0	Not visible	Not visible	A	14-29	22
			B	14-43	21
			C	14-71	25
			D	14-100	53
			E	13-64	24

4.3 Transmission Electron Microscopy

TEM images were taken and prepared at DOW Chemical and are shown in figure 4.2 below for the five porous samples. As in the SEM image, the dense sample showed no porosity.

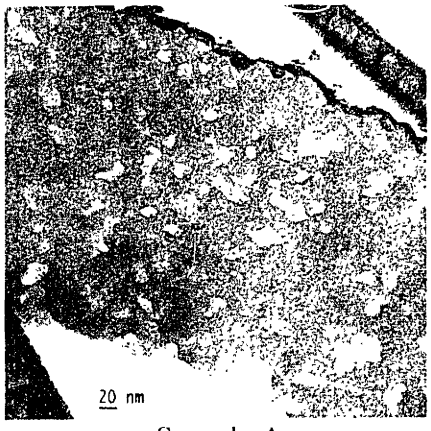

Sample A

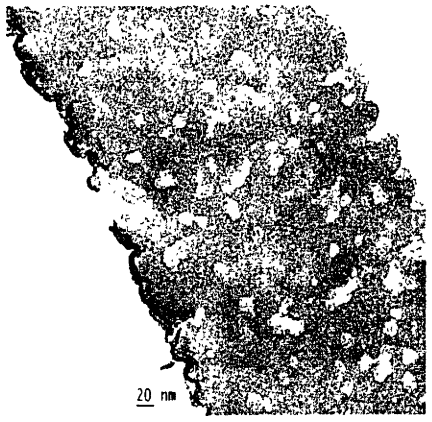

Sample B

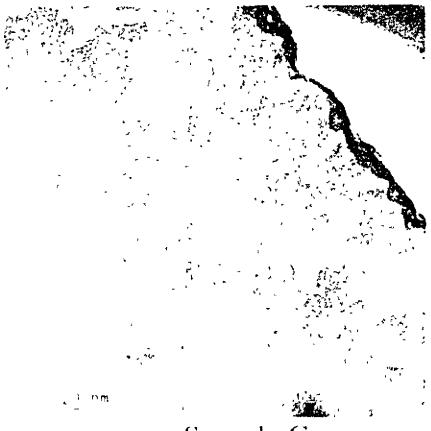

Sample C

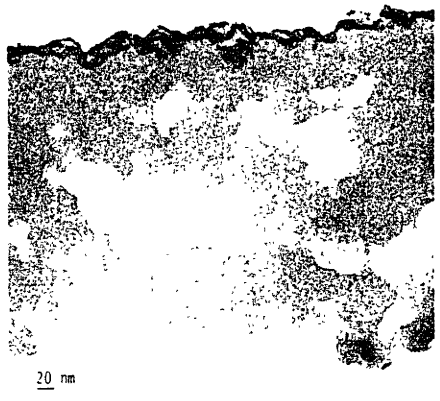

Sample D

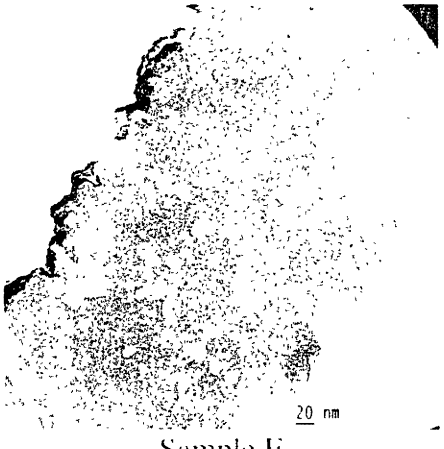

Sample E

Figure 4.2 TEM images for the six porous SiLK samples (A-E)

Table 4.3 compiles the manual pore size measurements for each sample from the previous TEM images.

Table 4.3 Manual pore size measurements for each sample from the previous TEM images.

Sample	Pore size range (nm)	Avg pore size (nm)	Sample	Pore size range (nm)	Avg pore size (nm)
Dense SiLK J			Trend Matrix (pSiLK v7)		
0	N/a	N/a	A	5.5-46	20
			B	7-52	19
			C	6.5-55.5	31.5
			D	13-99.5	45.5
			E	6-32.5	15

4.4 Positronium Annihilation Lifetime Spectroscopy

Sample 0, a silicon wafer coated with 950 nm SiO_2, 50 nm Si_3N_4, and approximately 3600 Å dense SiLK, was first analyzed using the PALS beam to determine the percentage of positrons able to form Ps as well as the intensity of the backscattered Ps. This backscattering parameter is not dependent on the internal structure of the film, but only its chemical composition since it is due to Ps forming along the surface and scattering off to annihilate in vacuum. It appears in the data as a peak at near vacuum lifetimes at a consistent intensity for polymers of similar composition. Assuming the porous SiLK matrix is identical to dense SiLK, this backscattering intensity can also be subtracted from data for the porous SiLK samples. Table 4.4 shows the lifetimes and intensities of these lifetimes for the dense sample at 2.1 keV, 3.1 keV, and 4.1 keV. Approximately 28% of positrons formed Ps in the film. The best fit for the raw data was achieved using POSFIT® software assuming a cubic, three dimensional structure, which generated a bimodal model corresponding to lifetimes of approximately 3 and 6 seconds, which corresponds to micropore sizes of 10-14 Å. This data is consistent with the free volume of a dense polymer matrix.

Table 4.4 Lifetimes and corresponding intensities for the dense sample at 2.1 keV, 3.1 keV, and 4.1 keV show a bimodal distribution of pore sizes with peaks at 3 and 6 ns.

Beam energy (keV)	τ (ns)	I (%)	τ (ns)	I (%)
2.1	3.25 ± 0.07	21.3	6.48 ± 0.37	4.53
3.1	3.01 ± 0.08	20.8	5.79 ± 0.24	6.98
4.1	2.72 ± 0.08	17.2	5.19 ± 0.15	9.77

The backscattering component intensity was found to be inversely related to the beam energy, consistent with the fact that more Ps is formed at the surface at lower beam energies as seen in Table 4.5. The larger this backscattering intensity, the larger the error introduced into the pSiLK analysis, as more data is lost.

Table 4.5 The backscattering component intensity was found to be inversely related to the beam energy, consistent with the fact that more Ps is formed at the surface at lower beam energies.

Beam energy (keV)	τ (ns)	I (%)
2.1	130.5 ± 3.4	1.62
3.1	128 ± 4	1.13
4.1	130.4 ± 4.9	0.89

The porous samples were then analyzed using the same beam energies. In these porous films, a bimodal model was once again used with lifetime peaks in the mesopore range (10 ns –121 ns) shown in Table 4.6. The backscattering component was subtracted from the mesopore components of the fitted data, and micropore lifetimes were ignored as they were consistent with the dense matrix.

Table 4.6 In these porous films, a bimodal model was once again used for lifetime peaks in the mesopore range (10 ns –121 ns).

Sample	Beam energy (keV)	τ (ns)	I (%)	τ (ns)	I (%)
A	2.1	34 ± 5	1.20	106 ± 3	2.86
	3.1	45 ± 6	1.12	104 ± 4	2.81
	4.1	39 ± 8	0.85	101± 5	2.15
B	2.1	45 ± 5	1.45	111 ± 4	2.59
	3.1	30 ± 5	0.99	100 ± 2	3.25
	4.1	22 ± 5	1.01	98 ± 3	2.56

Table 4.6 continued In these porous films, a bimodal model was once again used for lifetime peaks in the mesopore range (10 ns –121 ns).

Sample	Beam energy (keV)	τ (ns)	I (%)	τ (ns)	I (%)
C	2.1	66 ± 9	1.41	134 ± 8	2.53
	3.1	55 ± 9	1.28	134 ± 7	2.8
	4.1	41 ± 8	0.68	122 ± 4	2.41
D	2.1	43 ± 9	0.46	142 ± 3	2.63
	3.1	27 ± 7	0.46	140 ± 2	2.73
	4.1	20 ± 10	0.33	135 ±2	2.16
E	2.1	35 ± 5	1.04	104 ± 3	3.13
	3.1	29 ± 5	1.06	99 ± 2	3.31
	4.1	32 ± 6	0.82	100 ± 3	2.4

4.5 Atomic Force Microscopy

AFM images were taken of two of the seven samples as a preliminary judge of the technique's effectiveness in measuring bulk film porosity (Figure 4.3). The images showed a difference in RMS possibly corresponding to different pore diameters, but surface morphology may not represent bulk porosity. Table 4.7 below shows the data from these two samples.

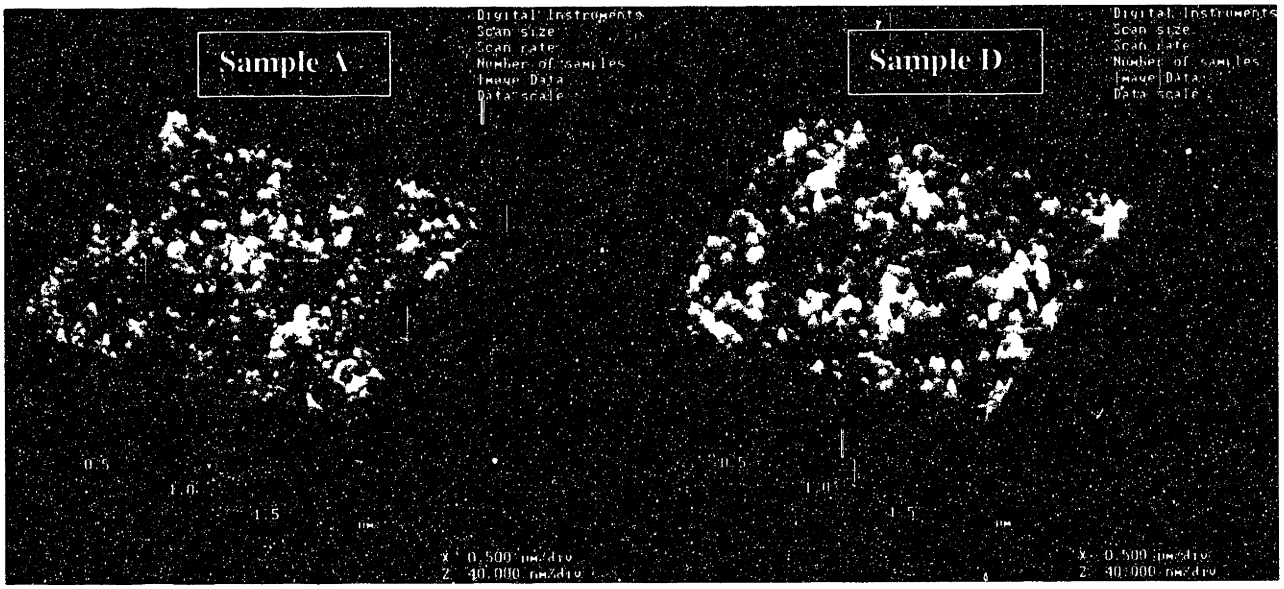

Figure 4.3 AFM images of Samples A and D showed a difference in RMS possibly corresponding to different pore diameters, but surface morphology may not represent bulk porosity.

Table 4.7 Data from AFM images, namely root mean squared distance measured on SiLK surface.

Sample	Root Mean Squared Distance (nm)
Dense SiLK J	0.7
A (porous SiLK)	2.383
D (porous SiLK)	2.788

4.6 X-Ray Reflectivity

XRR was used to determine the density, internal roughness, and thickness of the porous film. A sample raw data graph for sample A is show in figure 4.4. Table 4.8 shows the converted data, using Rigaku® software for each sample using this raw data.

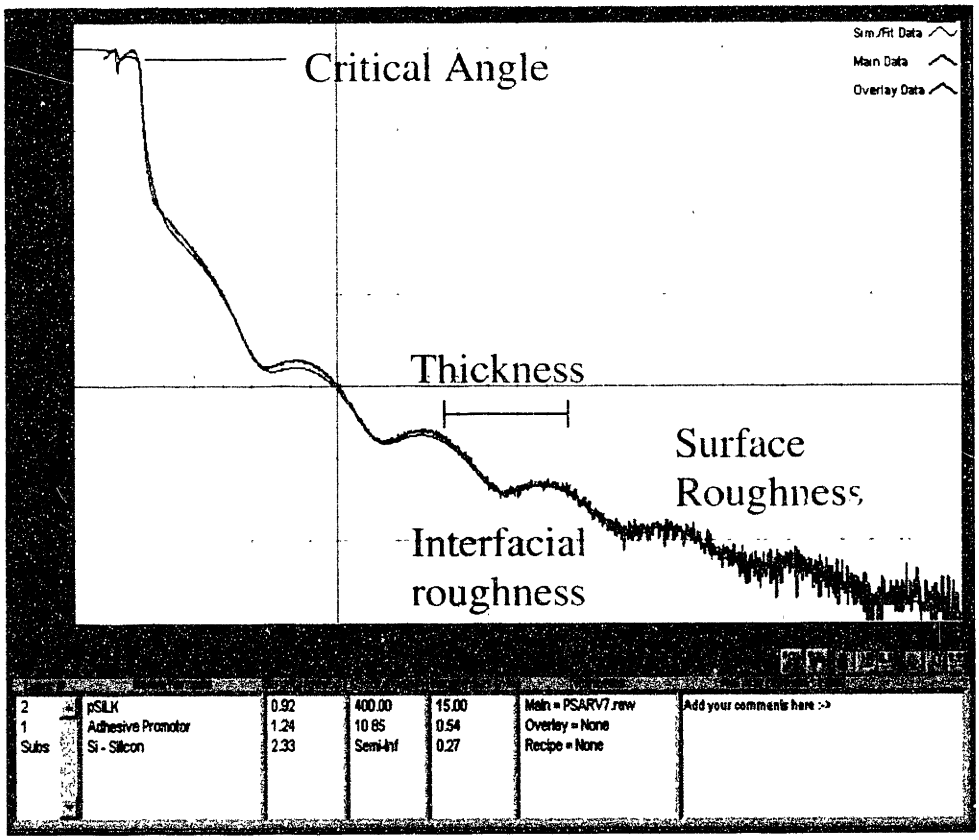

Figure 4.4 A sample output graph of reflectance angle (degrees) vs. Reflectivity (intensity).

Table 4.8 Density, thickness, and internal roughness measurements on porous SiLK using XRR.

Sample	Density (g/cm^3)	Thickness (Å)	Internal Roughness (nm)
0 (dense SiLK J)	1.07		
A	0.94	313.96	3.65
B	0.98	312.76	3.48
C	0.95	316.55	3.92
D	0.92	326.38	4.50
E	0.97	313.29	4.05

4.7 Capacitance Measurement

Capacitance data from the mercury probe was converted to κ values and are listed in Table 4.9.

Table 4.9 Dielectric constant values for each of the SiLK samples.

Sample	κ value	Sample	κ value
Dense SiLK J		Trend Matric (pSiLK v7)	
0	2.7	A	2.29
		B	2.26
		C	2.19
		D	2.09
		E	2.26

5. Discussion

5.1 Optical Methods

Refractive Index data can be correlated most directly to porosity changes in the film since a change in refractive index reflects a change in void fraction. The overall RI of the porous SiLK is a weighted average of the RI of voids (air n=1), and of the dense SiLK matrix (n~1.55). Therefore a change in porosity (or void fraction), should cause a change in the overall RI. Research has already been shown with other thin films that refractive index can be used to determine porosity in the film. [Srivasta] Pore size, however, is not so easily extracted from the data, as seen in Figure 5.1.

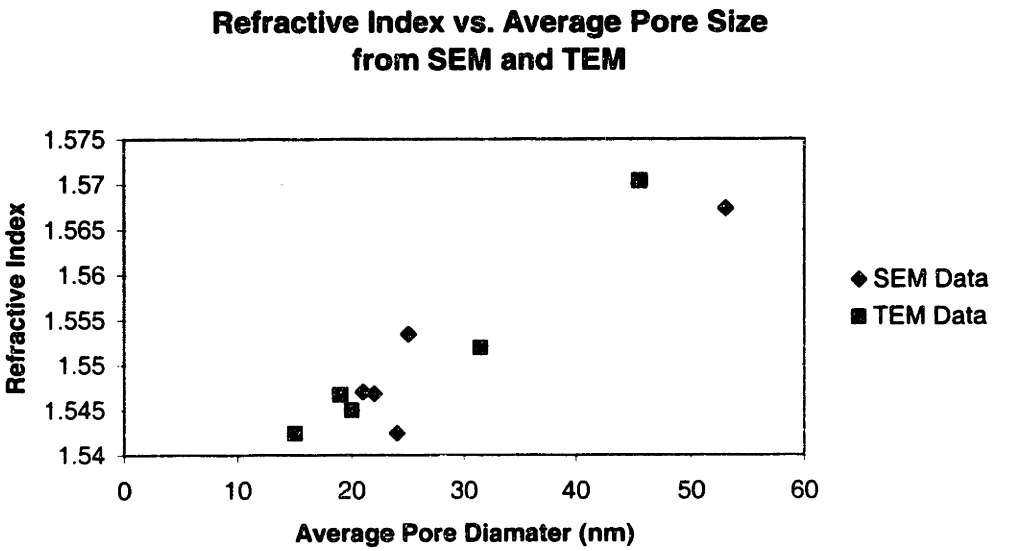

Figure 5.1 Increasing trend is qualitative in a graph of refractive index versus average pore size, but no quantitative relationship is clear.

Qualitatively, the samples with larger pores also have increased indices of refraction, but quantitatively the data does not seem to follow a specific trend. The quantitative relation cannot be established with this set of samples, since processing conditions may have affected other variables such as the degree of cross-linking. This data suggests problems with future repeatability of this experiment. The qualitative trend is significant, however, and can serve as an indicator for pores with diameter above 25 nm, which would cause the most damage to barrier films and further integration.

5.2 Scanning Electron Microscopy

The pore size limit of detection using a SEM is approximately 15 nm as shown from the results gathered. In order to determine pore size from a SEM image, the sample must be cross-sectioned either horizontally or vertically. This process using a focused ion beam (FIB) can sometimes cause a bright border around a pore, obscuring the real diameter, as seen in figure 5.2.

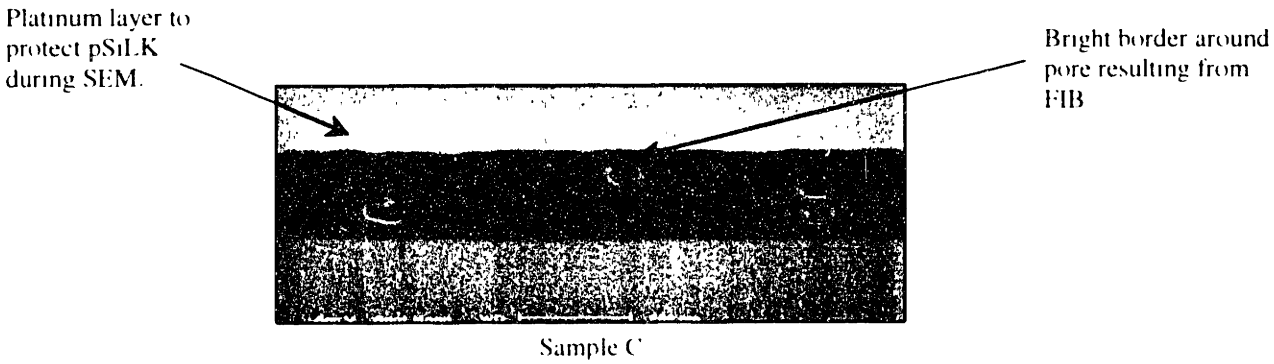

Figure 5.2 An example of a bright border, obscuring the actual surface of the pore in an SEM image.

These cross-sections are also random chords of pores, so it is unclear which, if any, represent the diameter of the pore. The samples are also coated with platinum or gold during preparation, which can affect surface porosity.

SEM images can also be used to determine local porosity by taking the area of voids divided by the area of film. The pores in this experimental version of porous SiLK are not spherical, however, making this measurement an approximation.

5.3 Transmission Electron Microscopy

The pore size limit of detection using a TEM is approximately 4nm as shown from the results gathered. Sample preparation for a TEM image involves microtoming, as well as also using a focused ion beam, both processes which can cause damage to the sample. Due to microtoming, the samples are very thin, and much more detail can be seen in the image, it is unclear which plane a pore lies in as in figure 5.3, and smaller pores can superimpose to create the image of a larger pore.

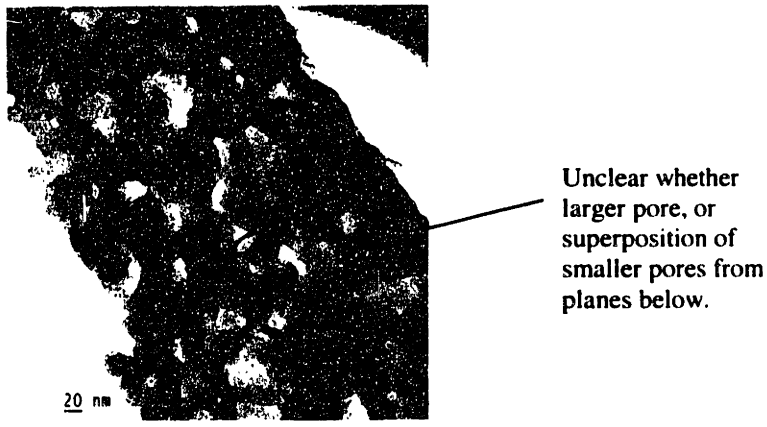

Figure 5.3 Sample TEM demonstrating difficulty in reading image. It is unclear whether larger pore, or superposition of smaller pores from planes below.

As when using an image from SEM analysis, local porosity can also be determined from a TEM image. The problems arising from this experimental version of porous SiLK also apply in TEM, however, since the pores are not very spherical. Interpreting TEM images is consistently challenging amongst amorphous insulators. [Gidley]

5.4 Positronium Annihilation Lifetime Spectroscopy

In order for samples to be analyzed using the PALS technique, positronium (Ps) must be able to form in the material, and these Ps must be able to diffuse into the porosity. For the latter reason, interconnected pores must be capped, trapping Ps in the pores, to determine an average pore size. [Dull] In organic materials, the electron concentration is relatively low, but a relatively high percentage of positrons formed Ps in the porous SiLK compared to other polymers. The latter two criteria were also satisfied by porous SiLK, as the pores were dispersed throughout the matrix, and had a closed, approximately spherical pore geometry.

The raw data from a PALS beam can be converted from lifetimes to mesopore diameters referencing a chart compiled empirically. Table 5.1 includes the mesopore diameters for the varying process conditions.

Table 5.1 In these porous films, a bimodal model was once again used for lifetime peaks in the mesopore range (3 nm –20 nm).

Sample	Beam energy (keV)	Mesopore diameter (nm)	Mesopore diameter (nm)
A	2.1	2.9 ± 0.3	14.5 ± 1
	3.1	3.4 ± 0.4	13.5 ± 2
	4.1	3.2 ± 0.5	12.3 ± 2
B	2.1	3.6 ± 0.4	17.3 ± 2
	3.1	2.7 ± 0.3	12.1 ± 0.6
	4.1	2.3 ± 0.3	11.3 ± 1
C	2.1	5.3 ± 1	77 ± 30
	3.1	4.3 ± 1	77 ± 30
	4.1	3.3 ± 0.5	28.5 ± 4
D	2.1	3.4 ± 0.5	Vacuum
	3.1	2.5 ± 0.3	Vacuum
	4.1	2.2 ± 0.5	88 ± 20
E	2.1	3.0 ± 0.3	13.5 ± 1
	3.1	2.7 ± 0.2	11.6 ± 0.6
	4.1	2.8 ± 0.3	12.1 ± 1

The dense sample did not show any pores in the mesopore range (2nm<d<50nm), but only pore diameters in the micropore range, (d < 2nm) which are due to the volume fraction of voids in the dense polymer matrix. Pores in the micropore range were consistent, however, between all porous and dense samples, implying a very similar dense polymer compromising the matrix. The data shows a slight decrease in pore size with increased implantation depth. This trend is unclear, however, as it may be due to the increased amount of backscattering at lower implantation depths. As the pore size approaches 20 nm, however, the lifetimes are approaching those of values at vacuum (142 ns), and resolution decreases exponentially.

These pore sizes were then correlated to data from optical measurements to determine the effects of this smaller range of pore size on the film refractive index. The qualitative trends follow very closely those from analysis with the SEM, as shown in Figure 5.4.

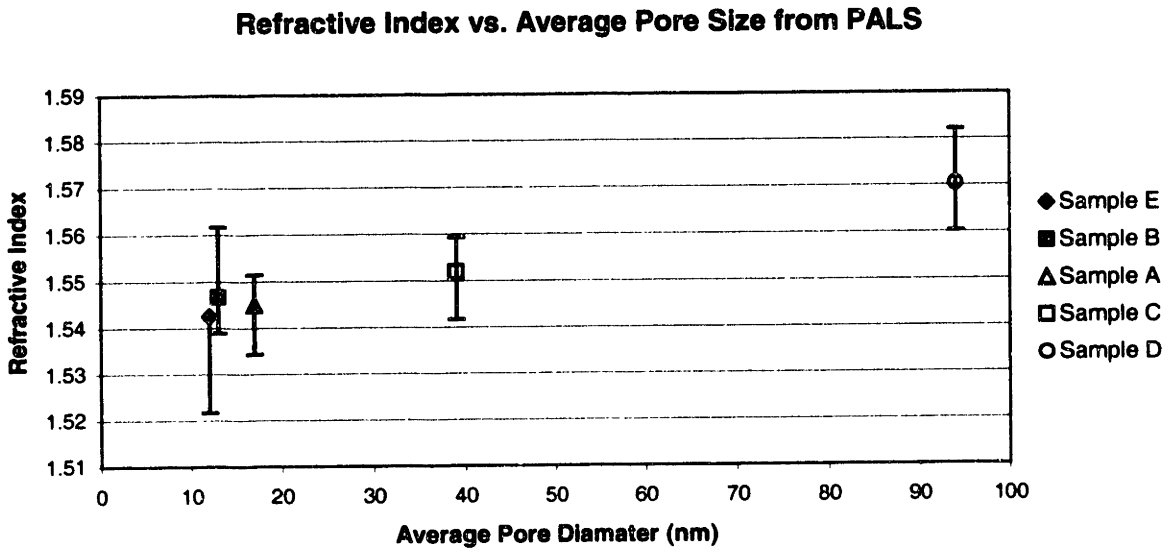

Figure 5.4 The qualitative trends between refractive index and pore diameter using PALS are very similar to those from analysis with SEM.

5.5 Atomic Force Microscopy

AFM analysis was only done on samples A and D, because data was inconclusive. Work has been done in the past with metals, in particular copper, to successfully determine grain sizes using AFM and the power spectral density function. This method could not be applied to pores on a porous SiLK surface, however, due to several considerations. AFM is a surface technique, so an assumption must be made that the surface is similar to the bulk of the material. This assumption is difficult to validate with spin on materials since the physics of spin on predicts that a thin dense layer may form at the surface of the film due to surface tension effects. Also the AFM tip is in contact with the film, which can result in smearing of the features due to the soft nature of the polymer relative to the cantilever tip.

5.6 X-Ray Reflectivity

Porosity can be calculated from the density values of a dense matrix and the porous version. The position of the critical angle in the raw x-ray data is used to

determine the density, shown in Table 5.2, and finally the porosity using the following equation:

$$P = 1 - (\rho_{porous}/\rho_{dense})$$

Table 5.2 Converted porosity data.

Sample	Porosity (%)	Sample	Porosity (%)	Avg Pore Size from SEM (nm)
0 (dense SiLK J)	0	A	12	22
		B	9	21
		C	11	25
		D	14	53
		E	9	24

Since the porogen loading for all samples was identical, there should be no variation in density, or porosity. There is no clear trend versus porosity or pore size from SEM, so this data oscillation may be due to resolution effects from the tool. This data can also be related to optical measurements to determine the correlation between refractive index and porosity of the film as shown in Figure 5.5.

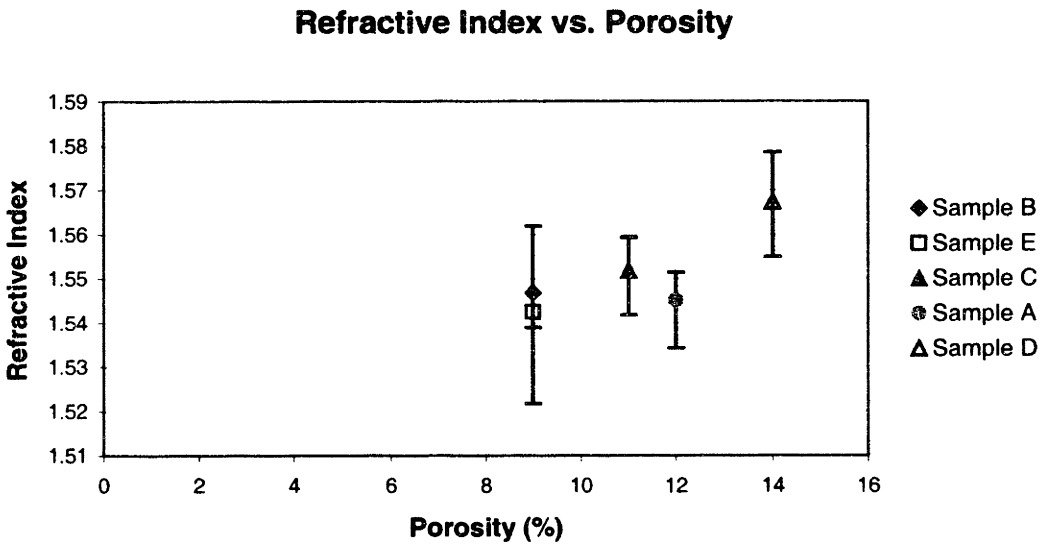

Figure 5.5 The relationship between refractive index and porosity is nonlinear, suggesting unintended changes in the polymer may have occurred due to processing.

The relationship between porosity and refractive index should be linear according to past studies. [Srivasta] The nonlinearity may be due to unintended effects from processing such as extra cross linking and pore aggregation. Error in measurement is

large, but sample D is statistically significantly higher in refractive index than the other samples.

Internal roughness can also be used as a qualitative measure of pore size, as seen from the correlation below in Figure 5.6.

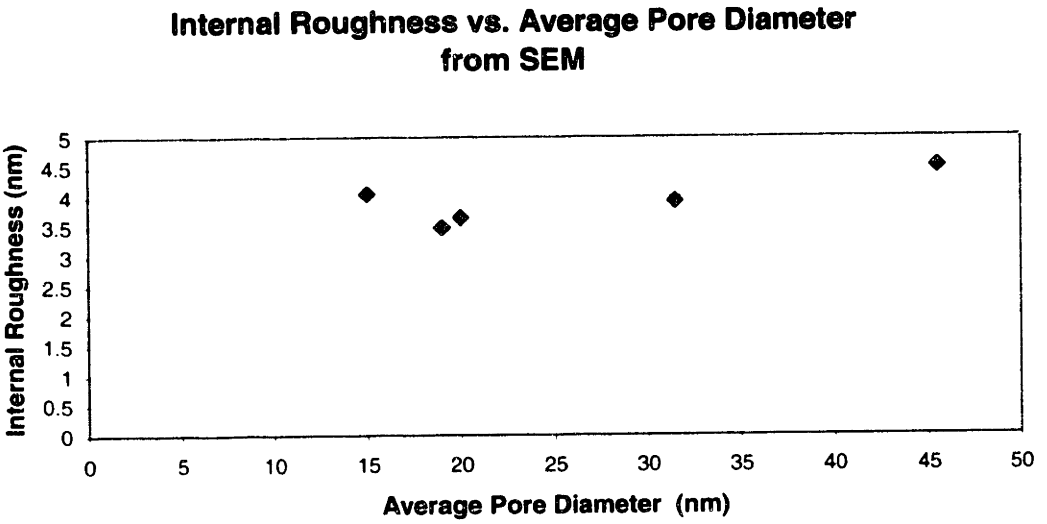

Figure 5.6 Internal roughness can also be used as a qualitative measure of average pore diameter, although the trend should be tested with other materials.

The slight upward trend falls above the sensitivity of the machine, but may also be affected by factors as a result of varied processing.

Organic films have a tendency to scatter x-rays weakly, but porous SiLK did not pose any problems gathering raw data. Certain samples were too rough internally to accurately determine the thickness, but values did not diverge too greatly from values determined by spectroscopic ellipsometry. [Collins]

5.7 Capacitance Measurement

The ultimate goal in bringing these low κ films into integration is to decrease the overall κ value of the insulating film stack. Measurements were finally taken on these experimental samples to determine if pore size or porosity have any direct correlation to the dielectric constant. This data is plotted in Figure 5.7 below.

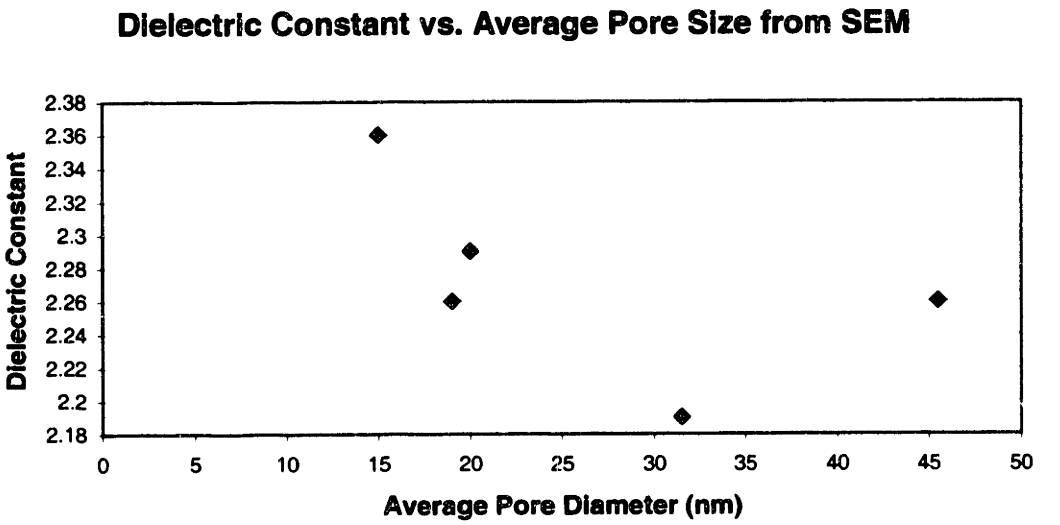

Figure 5.7 An increase in average pore size produces a decreased dielectric constant as well, contrary to theory which proposes that only porosity can affect the κ value.

All porous samples, regardless of processing showed lower dielectric constants than the original dense sample (κ ~ 2.65). The qualitative trend implies that the dielectric constant decreases as the average pore size increases. Theoretically there should be no relationship between pore size and dielectric constant if the porosity is held constant. This deviation may be due to larger pores creating a decreased contact area for the mercury probe, as the total dielectric constant is directly proportional to the mercury dot size.

6. Conclusions

Direct methods, such as Scanning Electron Microscopy and Transmission Electron Microscopy have long been the standard in porosity determination. Samples are prepared, often cross-sectioned, and viewed under an SEM or TEM. Artefacts can arise from sample preparation, but data is mostly reliable, as it generates a physical image. Due to resolution limitations, SEM can only accurately image pores above 15 nm, which lies above the upper limit for pore diameter in microelectronics fabrication. TEM can image smaller pores, but throughput is much too low for use as a fabrication inline monitor.

Although Positronium Annihilation Lifetime Spectroscopy is an indirect method, it would be useful for analysis of pores below the limits of TEM and SEM. Samples do not undergo any preparation, accept to remove any dust on the surface. Radiation sources

in a fabrication facility add complications, but efforts are underway to insulate this component of the tool, and make measurement time more efficient.

Optical tools calibrated for use with organic materials have been used for inline monitoring to control thickness and refractive index, and this data can be correlated to trends in pore size and porosity to be used as a qualitative monitor for an inline process. The optical data can then be referenced with pore size measurements from SEM for pore diameters greater than 15 nm, and PALS for pore diameters less than 15 nm. This correlation would need to run with the same set of samples for each technique to generate this correlation, since PALS data can be material dependent. Optical methods have not shown any particular disadvantages for use with organic materials, as they are mostly transparent polymers. Refractive index can also be calibrated to give porosity values with data from x-ray reflectivity measurements, which showed a direct relationship.

X-Ray Reflectivity measurements were used to determine the porosity of the films, as well as the thickness and internal roughness. This tool could perform both porosity and pore size evaluations if a relationship between internal roughness and pore size can be determined. Although such tools do not exist for use in a manufacturing fabrication environment, development is being pursued for this purpose. Experiments with porous SiLK showed no decreased intensity due to organic composition. Techniques such as ellipsometric porosimetry, small angle neutron scattering, and small angle x-ray scattering may also become very useful in analyzing such porous organics as solvents become readily available and more experiments are conducted.

Semiconductor fabrication requires a precise, controlled environment where timing is exact and future processes depend on every preceding step. Monitoring devices are necessary at every step to ensure the quality of each layer and ultimately the final device. As porous low κ materials become standard in manufacturing, porosity metrology will be integrated into the manufacturing line. Optical tools and a possible inline x-ray reflectivity tool would be optimal, since both techniques are commercially available, have proven high throughput, and can be clearly correlated to pore size and porosity in organic thin films.

7. References

Baklanov, M.R. Kondoh, E. Lin, E.K. Gidley, D.W. Mogilnikov, K.P. Sun, J.N. "Comparative Study of Porous SOG Films with Different Non-destructive Instrumentation." International Interconnect Technology Conference. 2001.

Baklanov, M.R. Mogilnikov, K.P. "Characterisation of Low-K Dielectric Films by Ellipsometric Porosimetry." Materials Research Society Symposium Proceedings. Volume 612. 2000. Pages D4.2.1-D4.2.12.

Bontempi, E. Depero, L.E. et al. "X-Ray Reflectivity Spectra of Ultrathin Films and Nanometric Mulitlayers Experiment and Simulation." Materials Research Society Symposium Proceedings. 2001.

Brown, A.J. et al. "The Kelvin Equation and Adsorption Hysteresis." in McEnaney, B. Characterisation of Porous Solids IV. Royal Society of Chemistry: Cambridge, UK. 1996. Pages 1-8.

Collins, R.W. "Spectroscopic Ellipsometry." in Ulman, A. Characterization of Organic Thin Films. Butterworth-Heinemann: Boston. 1995. Pages 35-56.

Dull, T.L. Frieze, W.E. Gidley, D.W. Sun, J.N. Yee, A.F. "Determination of Pore Size in Mesoporous Thin Films fro the Annihilation Lifetime of Positronium." Journal of Physical Chemistry B. Volume 105, Number 20. Pages 4657-4662.

Gidley, D.W. Frieze, W.E. Dull, T.L. Sun, J.N. Yee, A.F. "Probing Pore Characteristics in Low-K Thin Films Using Positronium Annihilation Lifetime Spectroscopy." Materials Research Society Symposium Proceedings. Volume 612. 2000. Pages D4.3.1-D.4.3.11.

Golden, J.H., Hawker, C.J. Ho, P.S. "Designing Porous Low-k Dielectrics." Semiconductor International. May, 2001. Pages 79-87.

Goworek, T. et al. "Mesopore Characterisation by Positron Annihilation." in Unger, K.K. Characterisation of Porous Solids IV. Elsevier: Amsterdam. 2000. Pages 557-565.

International Roadmap for Semiconductors, 2001 Edition: Interconnect.

Interuniversity Microelectronics Center (IMEC) Leuven, Belgium, courtesy of Hitachi Chemical Company, Limited, Japan.

Jain, A. et al. "Processing and Characterization of Silica Xerogel Films for Low-K Dielectric Applications." Materials Research Society Symposium Proceedings. Volume 565. 1999. Pages 29-40.

King, S.M. "Small Angle Neutron Scattering." in Pethrick, R.A. Dawkins, J.V. Modern Techniques for Polymer Characterisation, Chapter 7. John Wiley, 1999.

Lee, W.W. Ho, P.S. "Low-Dielectric-Constant Materials for ULSI Interlayer-Dielectric Applications." Materials Research Society Bulletin. October, 1997. Pages 19-27.

Lita, A. Sanchez, J.E. "Characterization of Surface Structure in Sputtered Al Films: Correlation to Microstructure Evolution." Journal of Applied Physics. Volume 85, Number 2 January 15, 1999. Pages 876-882.

Morgan, M. et al. "Structure-Property Correlation in Low K Dielectric Materials." Materials Research Society Symposium Proceedings. Volume 565. 1999. Pages 69-79.

Srivasta, A. Ygartua, C. "Spectroscopic Ellipsometry for Copper and Low κ Process Development." Yield Management Solutions. Spring 2000. Pages 52-56.

Sun, J.N. Gidley, D.W. Dull, T.L. Frieze, W.E. Yee, A.F. Ryan, T.E. Lin, S. Wetzel, J. "Probing Diffusion Barrier Integrity on Porous Silica Low-k Thin Films Using Positron Annihilation Lifetime Spectroscopy." Journal of Applied Physics. Volume 89. Number 9. May 1, 2001. Pages 5138-5144.

Toma, D. et al. "Ultra Low k Dielectric Materials and Technologies-Impact on Tool Development." In Low and High Dielectric Constant Materials: Materials Science, Processing, and Reliability Issues and Thin Films Materials for Advanced Packaging Technologies. The Electrochemical Society, Inc.: Pennington, NJ. 2000. Pages 5-10.

THESIS PROCESSING SLIP

FIXED FIELD: ill _____ name _____

index _____ biblio _____

▶ **COPIES:** Archives Aero Dewey Barker Hum

Lindgren Music Rotch Science Sche-Plough

TITLE VARIES: ▶ ☐ _____

_____

_____

NAME VARIES: ▶ ☐ _____

_____

IMPRINT: **(COPYRIGHT)** _____

_____

▶ **COLLATION:** _____

_____

▶ **ADD: DEGREE:** _____ ▶ **DEPT.:** _____

▶ **ADD: DEGREE:** _____ ▶ **DEPT.:** _____

SUPERVISORS: _____

_____

NOTES:

_____ cat'r. date:

page

▶ **DEPT:** _____

▶ **YEAR:** _____ ▶ **DEGREE:** _____

▶ **NAME:** _____

_____